

On a Novel Torque Detection Technique for Magnetorheological Actuators

Carlos Rossa, Laurent Eck, Alain Micaelli, and José Lozada

Abstract—This paper focuses on a new torque detection technique for magnetorheological (MR) actuators. An MR fluid consists of a suspension of ferromagnetic micron-sized particles in a carrier fluid. Under the action of a magnetic field, these particles form chains-like structures which interact with the magnetic poles. The torque detection technique is based on the assumption that a relative displacement of the poles stretches the chains, altering the magnetic reluctance of the fluid gap. This hypothesis is analytically developed using an elementary group of ferromagnetic particles placed in a non-magnetic carrier liquid. A measure of the excitation coil impedance using a high precision demodulator, is used to verify this hypothesis. Experimental results show that when the poles are displaced before the rupture of the chains, the chains are stretched and the reluctance increases. A higher sensitivity system is subsequently proposed to detect the variation of an external torque. The experimental results demonstrate that the system is able to detect the application as well as the release of the torque and can successfully be employed to detect the chain rupture critical point.

Index Terms—Magnetorheological actuator, embedded sensor, torque sensing, reluctance variation.

1. INTRODUCTION

A magnetorheological (MR) fluid is a suspension of soft ferromagnetic micron-sized particles (typically 1 to 10 microns) dispersed in a carrying liquid (mineral oil, synthetic oil or water). Their volume concentration in the fluid may range between 20% and 40% [2]. The action of a magnetic field alters rapidly, strongly and reversibly the rheological properties of these materials. The particles magnetization leads to the formation of chain-like structures or aggregates that are roughly aligned parallel in the direction of the magnetic field [3].

The necessary mechanical energy to break these structures increases with the strength of the applied magnetic field resulting in a field dependent yield stress. This is macroscopically perceived as a change in the viscous characteristics of the suspension, thereby restricting the displacement of the fluid.

When the fluid is confined between two magnetic poles, this phenomenon can be exploited for the design of variable impedance actuators. Such devices provide high controllability, fast response time, very low power requirements and high torque density, holding grate potential in many applications requiring controllable impedance such as clutches [4], brakes

The authors are with the French Atomic Energy Commission, CEA, LIST, Sensorial and Ambient Interfaces Laboratory, 91191 Gif-sur-Yvette, France. rossa@ualberta.ca; [laurent.eck; alain.micaelli}@cea.fr](mailto:{laurent.eck; alain.micaelli}@cea.fr); joselozada@uti.edu.ec

An earlier version of this paper was presented at the IEEE SENSORS 2012 Conference and was published in its Proceedings [1].

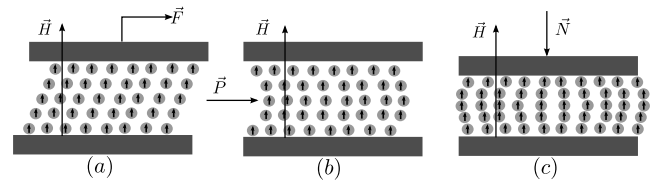


Fig. 1. Typical operation modes of MR fluids: On the shear mode (a) the fluid creates a resistive force against the pole velocity induced by an external force \vec{F} . On the valve mode (b) the magnetic field controls the resistance of the fluid flow due to the pressure drop ΔP . In the compression mode (c), a force \vec{N} is applied perpendicularly to the poles and the fluid resists against the normal displacement of the poles

[5], valves [6], dampers [7], actuators for robotics [8][9][10] and for haptics applications [11][12][13].

MR actuators can be classified according to three different operation modes: valve mode, direct shear mode or squeeze film compression mode [14], as schematically shown in Fig. 1. The magnetic field is typically provided by coils. The shear mode (a) is usually employed in the design of rotary brakes. In this case, two magnetic poles can be relatively displaced by the action of an external force. The chain-like structures create a resistive force against the pole velocity. In the valve mode (b), the poles are immobilized and the magnetic field strength controls the necessary pressure difference between the input and the output to induce a fluid flow. In the compression mode (c), a force acts perpendicularly to the poles and the necessary force to compress the gap is controlled.

The magnetic poles hydrodynamically interact with the particles [15] thus, when an external force induces a displacement of a magnetic pole or a fluid flow, the chains are stretched according to the motion [16] and the distance between neighbouring particles is modified. The separation of the particles by the non-magnetic liquid alters the magnetic environment in the fluid gap [17]. In other words, the reluctance perceived by the magnetic flux is altered. The magnetic reluctance is defined as the ratio of the magnetomotive force (in Amperes-turn) to the magnetic flux (in Webers) [18].

A measure of the magnetic reluctance variation in the fluid gap can be used as a direct indication of the chain-like structures arrangement and can therefore be associated to an external force. In this paper, a rotary MR brake operating in shear mode is used to investigate the variation of the reluctance when the chain like structures are stretched due to a relative displacement of the magnetic poles.

The paper is organized as follows. Section 2 presents a brief review of MR fluids behaviour. Subsequently, in Section 3, the reluctance variation assumption is developed using an elementary group of ferromagnetic particles placed in a non-

magnetic carrier liquid. Theoretical results demonstrate that when a chain of two isolated particles is stretched, a reluctance variation of 22% can be observed. Since the inductance of the excitation coil is inversely proportional to the reluctance, a measure of the impedance perceived by the coil is used to validate the reluctance variation assumption. A sinusoidal excitation voltage is sent to the brake and the phase difference between the voltage and the current is observed when the poles are displaced. This method is used as proof of concept to validate the concept and to exclude other phenomena that can generate a change in magnetic flux and that could erroneously be interpreted as a reluctance variation, such as eddy currents. This method requires relatively large displacement amplitude. In Section 6, a second method is developed. In this case the brake is equipped with two coils. The first one is used to generate a constant magnetic field. A flux variation, due to a change in the reluctance, induces a current in both coils which can be observed in the second one. The results demonstrate that the system reacts satisfactory to the action of an external force.

2. RHEOLOGICAL FLUID BEHAVIOUR

Fig. 2 shows a schematic view of the behaviour of an MR fluid placed between two magnetic poles submitted to an external force. Consider that the ferromagnetic particles are homogeneously placed in a carrier liquid (Fig. 2a). When a magnetic field \vec{H} is applied across the magnetic poles, the particles are magnetized and possess henceforth a magnetic moment aligned in the direction of the magnetic field (Fig. 2b). The magnetization of each particle depends on the applied field and on the disturbance fields emanating from the neighbouring magnetized particles [19]. The particles then behave as magnetic dipoles that undergo magnetic interaction forces (Fig. 2c). Hence, this mutual interaction amongst the particles causes the formation of chain-like structures or fibrils, roughly aligned parallel to the applied field (Fig. 2d). If the magnetic poles are considered as a magnetic potential surface, the interaction between a particle and the pole can be modelled as equivalent to the interaction of the particle and the dipole images of all other particles reflected about the surface [19]. Thus, the particle, when close to the wall, acquires the same translational velocity than the pole. According to Bossis *et al* [16], the chains are supposed to deform with the strain, thus the distance between two neighboring particles increases according to the motion up to rupture (Fig. 2e). The chains are subsequently continuously broken on the vicinity of the poles [20][21] and immediately reconstituted due to the field across the poles and due to the pole displacement (Fig. 2e, Fig. 2f).

In the absence of a magnetic field, MR fluids can be considered as a Newtonian fluid. When a field is applied, the magnetic interaction between the particles induces a magnetic force which is proportional to their relative position and orientation to the external field and the magnetic permeability of the carrier fluid [15]. As predicted by electromagnetic theory, there is a quadratic relationship between the applied field strength and the interaction force. The fluid displays a pre-yield regime, characterized by a viscoelastic response [22],

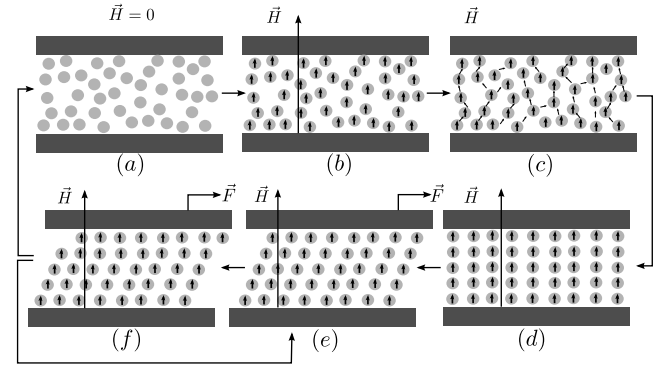


Fig. 2. Rheological effect in a magneto-rheological suspension between shearing plates: The particles are homogeneously distributed in the carrier liquid (a). A magnetic field is imposed (b), the particles are magnetized and behave as a magnetic dipole (c). They form then the chain-like structures aligned to the field (d). When the poles moves the chain structures are stretched and broken (e) and immediately reconstituted (f).

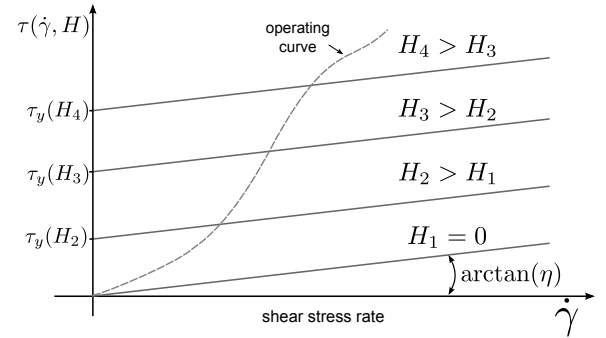


Fig. 3. MR fluid behaviour according to the Bingham plastic model. The fluid shear stress $\tau(\dot{\gamma}, H)$ is a function of the shear stress rate $\dot{\gamma}$ and of the field dependent yield point $\tau_y(H)$, where H_n is the magnetic field strength and η is the fluid viscosity coefficient. By controlling of the magnetic field, it is possible to follow almost any curve on this plan. This is the case of the dashed line which represents a fluid with a variable viscosity coefficient.

and a post-yield regime characterized by a viscous behaviour [23]. The transition point appears when the shear rate $\dot{\gamma}$ is zero.

The Herschel-Bulkley [24] and the Bingham formulations [25] are the plastic models commonly employed to describe the behaviour of MR fluids. The Herschel-Bulkley model considers a non-linear post-yield behaviour while Bingham model assumes a linear behaviour. The constitutive equation of the Bingham model is presented in Equation (1), where $\tau(\dot{\gamma}, H)$ is the shear stress and $\tau_y(H)$ is yield stress which depends on the magnetic field H . The shear strain rate and the fluid viscosity coefficient are denoted $\dot{\gamma}$ and η respectively.

$$\begin{cases} \tau(\dot{\gamma}, H) = |\tau_y(H)| + \eta|\dot{\gamma}| & |\tau(\dot{\gamma}, H)| \geq \tau_y(H) \\ \dot{\gamma} = 0 & |\tau(\dot{\gamma}, H)| < \tau_y(H) \end{cases} \quad (1)$$

Fig. 3 presents the evolution of the fluid shear stress as a function of the magnetic field according to the Bingham plastic model. The pre-yield regions are shortened when the magnetic field increases. During the pre-yield regime, or rather when $\tau(\dot{\gamma}, H) < \tau_y(H)$ and $\dot{\gamma} = 0$, the chain structures present a viscoelastic behaviour with some stiffness. The

common viscoplastic models used to describe this behaviour consider that the stiffness of the chains are almost negligible compared to their damping coefficient. If an external force is applied and induces a displacement of the poles, the chain structures are stretched and when the force is released the interaction between the particles tends to realign them with the magnetic field. When the fluid deforms beyond the yield point ($\tau(\dot{\gamma}, H) \geq \tau_y(H)$ and $\dot{\gamma} \neq 0$), its behaviour can satisfactorily be described by the Bingham model. The stiffness of the chain becomes proportional to the applied field.

Whatever the fluid regime (pre or post-yield), the stretching out of the chains are supposed to have the effect of altering the magnetic reluctance of the fluid. The analysis of the magnetic environment is focused during the deformation phase of the chains before their rupture. In order to associate the reluctance variation with the external torque, the following section presents a reluctance variation analysis between two ferromagnetic particles in a non-magnetic carrier fluid.

3. MAGNETIC RELUCTANCE VARIATION

In order to develop an analytical model that describes the reluctance variation as a function of the particles position, consider two isolated ferromagnetic particles in a non-magnetic carrier fluid, as presented in Fig. 4. Each particle with a diameter a is in a cubic volume of fluid measuring a^3 units. The center of each particle is separated by q units of a non-magnetic liquid, which possesses an absolute permeability μ_c . The absolute permeability of the particles is denoted μ_p . Note that the absolute permeability of the fluid is typically almost 2000 times inferior than the permeability of the particles.

The chains are in the initial position and the magnetic field induces a magnetic flux Φ_0 which is perpendicular to the poles (Fig. 4). The particles are then inclined from α radians and the magnetic flux is deviated (Fig. 4b). The magnetic flux when the chains are inclined is called Φ_1 .

The total reluctance of two particles is approximately calculated as follows:

$$\mathcal{R} = \frac{2}{a}\xi + \frac{q-a}{\mu_c a^2} \cos(\alpha) \quad (2)$$

where ξ is a constant depending only on the magnetic permeabilities given by:

$$\xi = \frac{4}{\pi} \frac{1}{\sqrt{\mu_p^2 + 2\mu_p\mu_c - 3\mu_c}} \arctan\left(\frac{1}{\sqrt{\mu_p + 3\mu_c}}\right) \quad (3)$$

The effective variation of the total reluctance as a function of the inclination angle α is computed as:

$$\delta\mathcal{R} = \frac{q-a}{\mu_c a^2} [1 - \cos(\alpha)] \quad (4)$$

Note that this amount of reluctance variation is given only between two isolated particles. Vicente et al. [26] developed a micro-rheological model of a magnetorheological fluid at low magnetic field strength by equalizing the torque exerted on a pair of particles by the external field and the hydrodynamic force by using the Stokesian friction approximation.

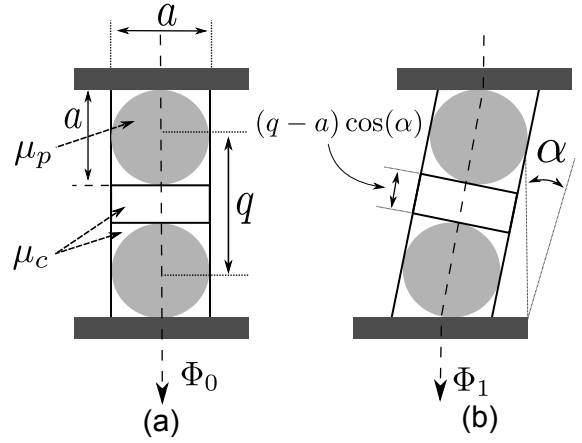


Fig. 4. Magnetic interaction between two isolated particles in a stretched chain structure. The center of each particles of a diameter a are separated by q units. The absolute permeability of the particle and of the carrier liquid are μ_p and μ_c respectively. The displacement of the poles stretches the chain-like structures which increases the magnetic reluctance. Where α is the inclination angle of the magnetic flux Φ .

Considering only the interaction between neighbouring particles, they obtained a critical rupture angle $\alpha = \alpha_c$ so that $\tan(\alpha_c) \approx \sqrt{1/2}$. This critical angle represents almost 22% of augmentation in the total reluctance when the single structure of Fig. 4 is stretched.

This analysis is only valid for an isolated chain of particles. For a representative volume of fluid, the particles interact with their neighbours and the variation of the total reluctance is considerably inferior. It has been demonstrated that the energy due to the interaction between the particles is lowest when the strain is zero [21]. Therefore, the formation of the chain structures aligned to the field corresponds to the lowest interaction energy in the gap. Since the magnetic energy increases with the reluctance, it can be concluded that all other arrangements of the chains results to an increased reluctance.

A rotary brake is used in order to validate this hypothesis and the results are presented in following sections.

4. TEST APPARATUS

A cross view of the miniature cylindrical brake used to validate the reluctance variation assumption is presented in Fig. 5. The fluid (Lord Corp. MRF-122EG) is placed in a gap g of 1mm separated by two concentric cylinders. The inner cylinder possesses a radius r_1 of 8mm and the outer radius r_2 is 9mm. The length $l = 25$ mm is the fluid gap length and the coil length is 10mm. No seal or bearing is mounted on the brake in order to reduce parasitic frictions forces.

The torque $T_b(t)$ developed by the brake can be separated into a field dependent torque $T_h(t)$ and a viscous torque $T_v(t)$ so that $T_b(t) = T_h(t) + T_v(t)$.

The controllable braking torque is given by the integral of the torque delivered by an elementary area dS at a given magnetic field H as:

$$T_h(t) = \int_{r_1}^{r_2} \int_0^{2\pi} r \tau_y(H) dr d\theta \quad (5)$$

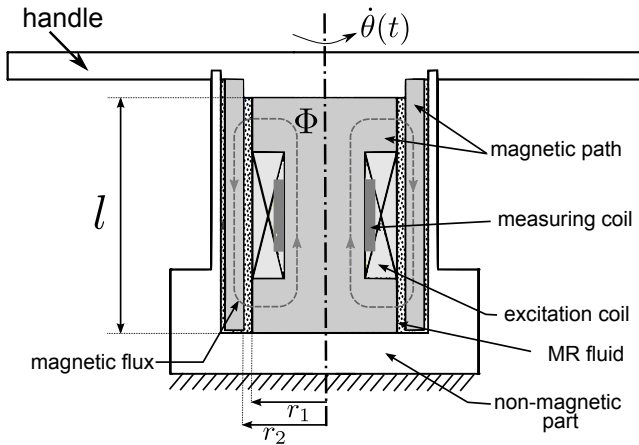


Fig. 5. Cross view of the miniature MR-based brake used to measure the reluctance variation in the fluid gap. The brake is formed by two concentric cylinders with a radius $r_1 = 8\text{mm}$ and $r_2 = 9\text{mm}$. The outer cylinder rotates according to a velocity denoted $\dot{\theta}(t)$. The height of both cylinders is $l = 25\text{mm}$. An excitation coil with 1000 turns and a measuring coil with 180 turns of wire are mounted around the axis. The magnetic flux is denoted Φ .

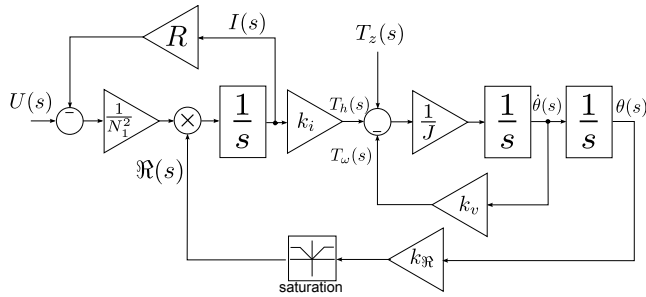


Fig. 6. Schematic representation of the MR brake. Considering only the excitation coil, which has N_1 turns of wire with a resistance R and perceives a reluctance $\mathcal{R}(s)$. When supplied by a voltage $U(s)$, it generates a current $I(s)$ that flows through the electromagnetic circuit resulting in a braking torque $T_h(s)$ where k_i and k_v are geometric constants. The viscous torque is called $T_v(s)$ and $T_z(s)$ is the external torque. The brake has an inertia J . The reluctance is assumed to be proportional to the position of the rotor $\theta(s)$. The saturation constraint represents the rupture of the chains. Beyond this point the reluctance is assumed to be constant.

The viscous torque $T_v(t)$ generated by the brake for a given velocity $\dot{\theta}(t)$ and a viscosity coefficient η is:

$$T_v(t) = 4\pi l \frac{r_1^2 r_2^2}{r_2^2 - r_1^2} \eta \dot{\theta}(t) \quad (6)$$

The relationship between the yield stress and the magnetic field can be approximated by $\tau_y(H) = \alpha H(t)^\beta$ where α and β are fluid index parameters [27] and $H(t)$ is a function of the current $i(t)$.

Thus, the total torque delivered by the brake can be rewritten as $T_b(t) = k_i i(t) + k_v \dot{\theta}(t)$ where k_i and k_v are two geometric constants. k_v depends on the fluid viscosity. A detailed modelling of a cylindrical brake is presented by Huang *et al.* [28].

The brake is equipped with two independent coils, called excitation coil and measuring coil. The excitation coil has $N_1 = 1000$ turns of wire corresponding to a measured inductance $L_1 = 9.39\text{mH}$. The inductance of the measuring is $L_2 = 132.7\mu\text{H}$ with $N_2 = 180$ turns of wire. The first one is supplied by a constant voltage in order to generate the

magnetic flux $\Phi(t)$. The variation of the magnetic flux across the magnetic circuit induces a current in the coils proportional to $d\Phi(t)/dt$ which can be used to observe the flux variation.

A simplified block-diagram of the brake is presented in Fig. 6, where only the excitation coil is represented. The voltage $U(s)$ induces a current $I(s)$. When an external torque is applied, it induces a relative displacement that alters the magnetic reluctance up to the rupture point of the chains.

The relationship between the excitation voltage $u(t)$ and the current $i(t)$ is:

$$u(t) = Ri(t) + N \frac{d\Phi(t)}{dt} \quad (7)$$

Where R is the electric resistance. Considering a single coil, the magnetic flux can be expressed as a function of the magnetomotive force by $\Phi(t) = Ni(t)/\mathcal{R}_t$, where \mathcal{R}_t is the total reluctance of the electromagnetic circuit. Combined to the previous equation, the relationship between the voltage and current in the coil is given by the transfer function $W(s)$ as:

$$W(s) = \frac{I(s)}{U(s)} = \frac{\mathcal{R}_t}{N^2 s + R\mathcal{R}_t} \quad (8)$$

The inductance L of the coil is defined as a function of the magnetic reluctance so that $L = N^2/\mathcal{R}_t$.

These equations suggest that there is two ways to observe the variation of the reluctance in the fluid gap:

- The voltage-to-current gain and its phase difference can be considered as the image of the reluctance, since the inductance of the coils is inversely proportional to the magnetic reluctance.
- The image of the derivative of the reluctance can be associated to the induced current in the coil. Indeed, a reluctance variation generates a flux variation, which can be observed as an induced current in the coils.

The first solution allows for a direct measurement of the reluctance and excludes disturbances from flux variation, due for example to eddy currents induced by the rotation of the brake. Although this solution can validate of the reluctance variation assumption and can be used as proof of concept, it requires relatively high displacement amplitudes and has not sufficient sensibility to detect external torques. The second solution can therefore be considered. It consists in observing a magnetic flux variation due to a change of the magnetic reluctance. This method provides higher sensibility and can be employed to detect external forces, but is not sufficient to verify the reluctance variation assumption. Therefore, these two solutions turn out to be complementary, and both are treated in the following sections.

5. PROOF OF CONCEPT

In this section, the reluctance variation assumption is validated using a measure of the impedance of the excitation coil. From equation (8) the voltage-to-current gain $G(j\omega)$ and the phase difference $\psi(j\omega)$, for a given frequency ω , are:

$$G(j\omega) = -10 \log \left(\frac{N^4}{\mathcal{R}_t^2} \omega^2 + R^2 \right) \quad (9)$$

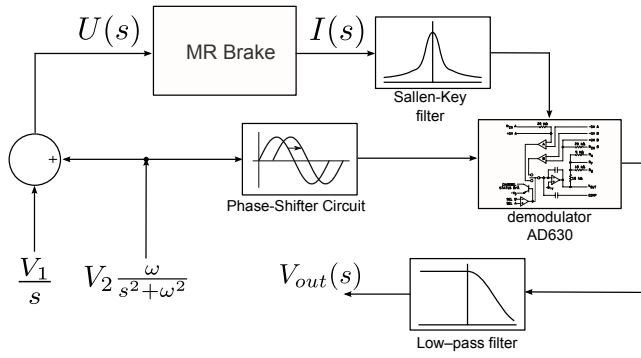


Fig. 7. Circuit used to measure the impedance of the coil. The brake is activated by a constant voltage V_1 in order to allow the chain-like structures to be formed. To this current a sinusoidal waveform V_2 of 10kHz is added. The current $I(s)$ then is measured and filtered to be compared with this excitation voltage. The DC level of the output $V_{out}(s)$ is a direct indication of the phase and of the amplitude of the current.

$$\psi(j\omega) = -\arctan\left(\frac{R}{N^2} \mathcal{R}_l \omega\right) \quad (10)$$

The amplitude of the measured current as well as its phase difference are a function of the magnetic reluctance and of the frequency. The reluctance has no influence on the current in permanent regime: The resultant current is given by $\lim_{t \rightarrow \infty} w(t) = \lim_{s \rightarrow 0} W(s)s$ and for voltage step function $U(s) = 1/s$ it yields $i(t) = 1/R$.

The brake is excited with a constant voltage V_1 , in order to generate a magnetic flux. To this voltage, a sinusoidal waveform V_2 of 10kHz is modulated. The phase difference between this signal and the measured voltage is proportional to the reluctance. A frequency demodulator AD630 is used as a precise phase comparator.

The voltage input is:

$$U(s) = \frac{1}{s} V_1 + \frac{\omega}{s^2 + \omega^2} V_2. \quad (11)$$

This excitation voltage generates both a constant current and a sinusoidal current measured using a shunt resistance of 1Ω . A schematic representation of the demodulator is shown in Fig. 7. In order to observe only the sinusoidal induced current, the measured current is filtered using a band-pass Sallen Key filter centered at 10kHz. Both filtered current and sinusoidal voltage signals constitute the input of the demodulator. The sinusoidal excitation voltage passes through a phase shifter circuit in order to reduce its phase difference with respect to the observed current. Failing that, both signals may possess a phase difference at least of $\pi/4$ and the phase difference due to the reluctance variation may not be observable.

The output DC level is proportional to the signals amplitude V_2 and $I(s)$ and phase difference between them. If one signal amplitude is constant, the output V_{out} is a direct indication of the phase. When these inputs are $\pi/2$ rad out of phase, the DC output is zero. The output is filtered by a low pass filter with a cutoff frequency of 5kHz. The output voltage $V_{out}(s)$ demodulator is the image of the arrangement of the chain-like structures.

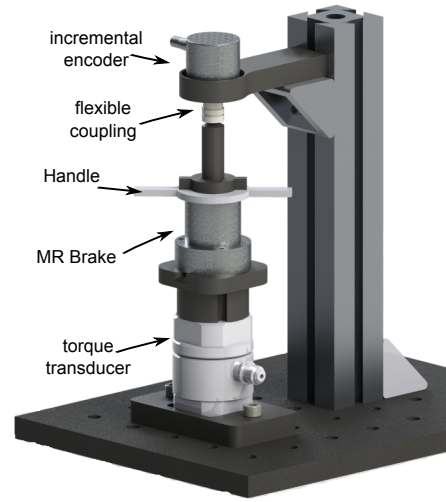


Fig. 8. Experimental validation test bench. The MR brake is placed over a torque transducer. The rotor is linked to a incremental encoder of 4096ppr through a flexible coupling.

5.1 Experimental Validation

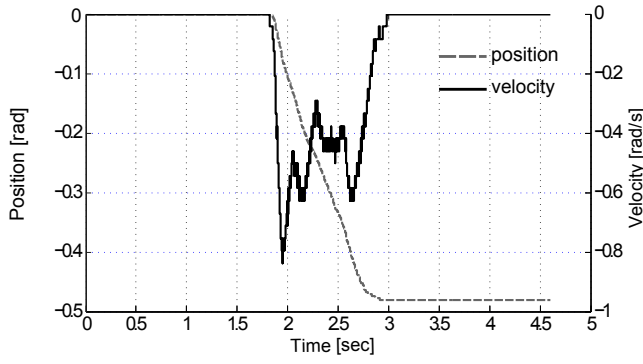
The brake was placed on the test bench shown in Fig. 8. It is composed of an incremental encoder with 4096 pulses per revolution and a torque transducer (Sensor development 01324) in order to measure the rotor position and the braking torque, and to correlate the change of the reluctance with the applied torque at the handle.

The excitation voltage is sent to the brake and its axis is manually turned to the right.

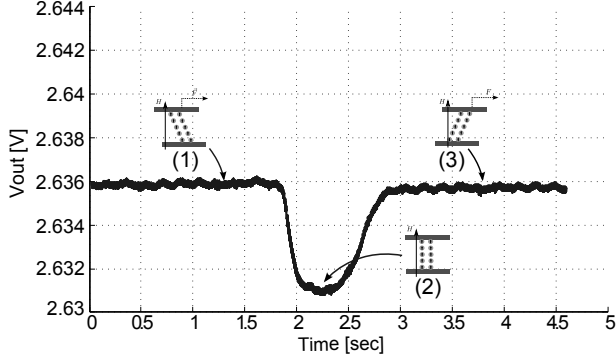
The experimental results are presented in Fig. 9. At the initial position the chains are already inclined to the right (point 1 in Fig (b)). An external torque is applied at the handle at $t=1.7s$. When the shaft rotates, the chains follow the displacement of the poles. The demodulator output decreases and reaches its minimum level at $t=2.1s$. It indicates that the chains are perpendicularly aligned with the poles (2 in Fig (b)). At this point the chains begin to be inclined in the other direction and at $t=2.7s$ the voltage returns to its initial value (point 3). The reluctance variation was observed during a total angular displacement of 12 degrees.

The demodulator output depends on the signal amplitude of the excitation voltage, maintained constant, and on the induced current. The relationship between the voltage and the current, obtained by Equation (9) is inversely proportional to the reluctance. The maximum level of the output is observed when the chains are stretched. It corresponds to the point where the impedance of the system reaches its lowest value. Since the inductance is inversely proportional to the reluctance, it can be concluded that the reluctance increases when the chains are stretched.

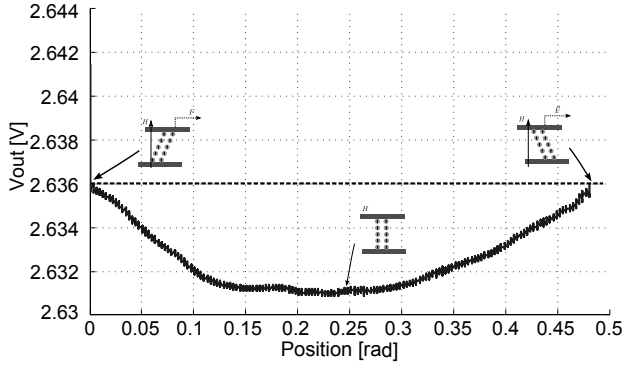
Although this method is a proof of concept, it is able only the detection of relative large displacement of the magnetic poles. A second method, based on the variation of the reluctance, is therefore performed in the following section.



(a) Rotor position and velocity



(b) Demodulator output versus time



(c) Demodulator output as a function of the rotor position

Fig. 9. Experimental results using the signal demodulator in order to observe the variation of the impedance of the coil. The reluctance of the fluid gap changes as a function of the position. The evolution of the chain-like structures is represented by two parallels shearing plates. The output of the system V_{out} is proportional to the magnetic reluctance. Fig. (a) presents the position and the velocity of the rotor, Fig. (b) shows the temporal evolution of the demodulator output and in (c) the output as a function of the position.

6. APPLICATION TO TORQUE DETECTION

In this section, the reluctance variation is observed using both coils. It is based on the induced current due to the magnetic flux variation. This current can then be associated to the derivative of the magnetic reluctance and allows for the implementation of higher circuit gains compared to the proof of concept providing thereby higher sensibility.

For the following equations $U_1(s)$, R_1 , $I_1(s)$ and $U_2(s)$, R_2 , $I_2(s)$ are the voltage, the electric resistance and the current of the excitation coil and the measuring coil respectively. The voltage of the coils as a function of the magnetic field given

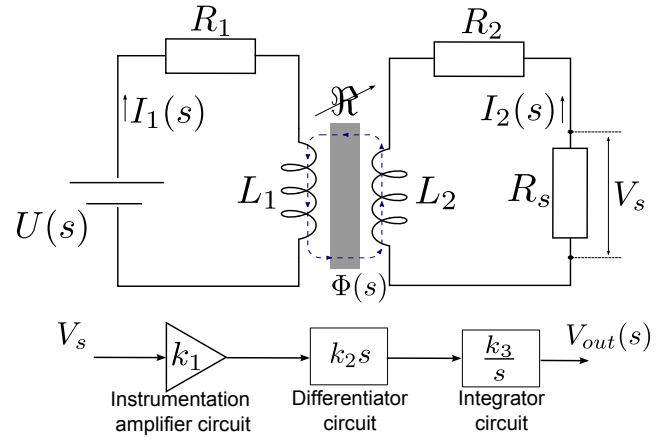


Fig. 10. Equivalent electromagnetic circuit comprising an excitation coil supplied by a constant voltage and a measuring coil. The derivative of the magnetic flux induces a current on the coils. In the measuring coil this current is observed as a voltage V_s across the shunt resistance R_s . This voltage is subsequently amplified and can be associated as the image of the derivative of the reluctance.

by Equation 7 yields:

$$U_1(s) = R_1 I_1(s) + N_1 \Phi(s) s \quad (12)$$

$$U_2(s) = R_2 I_2(s) + N_1 \Phi(s) s \quad (13)$$

Assuming an ideal transformer model (all flux generated by the excitation coil is supposed to link all the turns of every winding, including itself), the mutual magnetic field $\Phi(s)$ is computed as:

$$\Phi(s) = \frac{N_1 I_1(s) - N_2 I_2(s)}{\mathcal{R}_t} \quad (14)$$

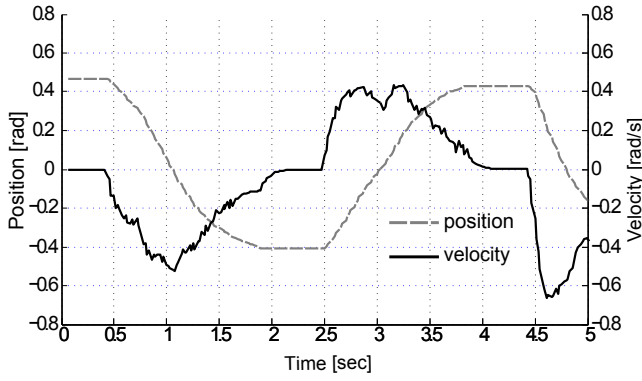
The schematic representation of the equivalent electric circuit is shown in Fig. 10. The induced current I_2 in the measuring coil is observed as a voltage across a shunt resistance called R_s . This voltage is amplified by means of an instrumentation amplifier according to a gain k_1 and attains the microvolts. A second gain is implemented using a differentiator and an integrator circuit in series, associated to a gain k_2 and k_3 respectively. The output voltage is computed as:

$$V_{out}(s) = k_1 k_2 k_3 I_2(s) R_s \quad (15)$$

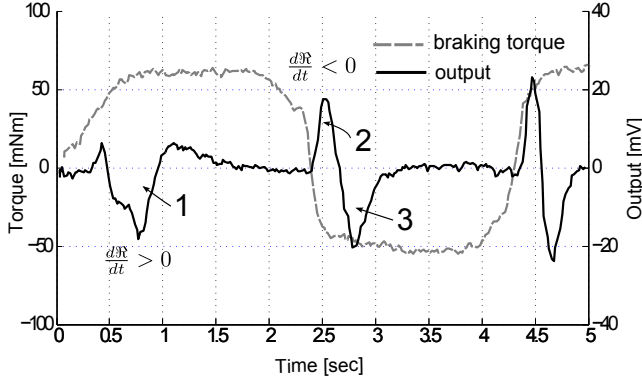
This circuit was previously validated using an U-shaped variable reluctance magnetic core.

6.1 Experimental Results

For torque detection, two different tests are conducted. The first realised in a dynamic dynamic case with an oscillatory velocity of the rotor, demonstrates the feasibility of the proposed method. In the second case, the velocity of the rotor is almost zero. In both cases, a torque is manually imposed at the handle and the evolution of the measured torque and the output voltage are simultaneously monitored. A constant voltage is sent to the excitation coil in order to activate the brake.



(a) Rotor position and velocity

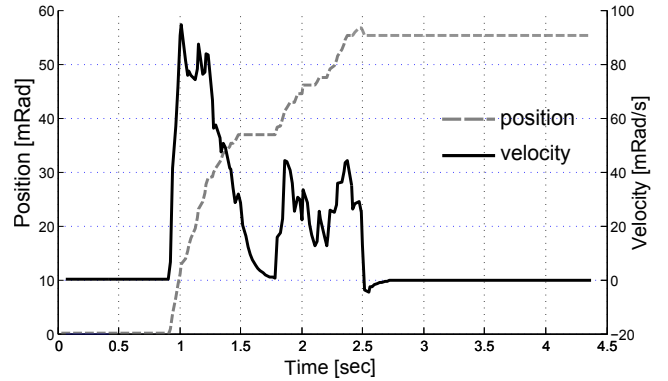


(b) Demodulator output and the applied torque

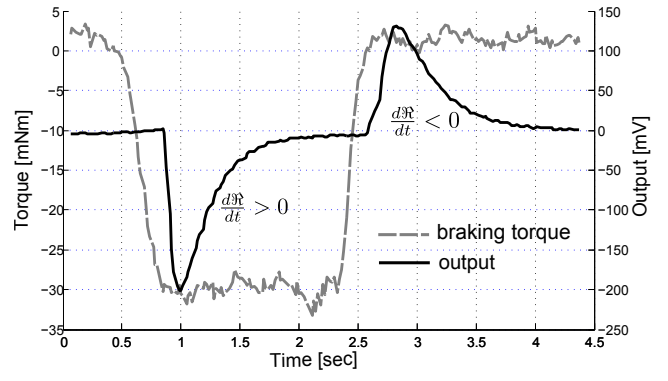
Fig. 11. External torque variation detection observing the magnetic flux. A torque is applied in both direction at the handle and the displacement of the poles stretches the chains (a). It is observed in (b) as negative voltage (1) and (3), and as a positive (2) voltage which characterizes an augmentation and a diminution of the observed reluctance. When the reluctance does not change, the output voltage returns to zero. The observed coulomb friction is 30mNm.

Fig. 11 presents the experimental results in dynamic case. During the inclination of the chains, a negative voltage appears in the measurement circuit ($t=0.7s$) which characterizes a reluctance augmentation (point 1). The torque is maintained until $t=2.3s$ and then inverted. The reluctance decreases until the chains are aligned with the field and then raises again while the chains are inclined in the other direction by the displacement of the pole. This behaviour is observed as a positive voltage (point 2) followed by a negative voltage (point 3) representing the diminution and augmentation of the reluctance respectively. When the chains do not move, the output voltage returns to zero. It demonstrates that the reluctance variation is observed only before the rupture of the chain structures.

The second experiment aims to observe the evolution of the output voltage as a function of the torque in quasi-static regime. Fig. 12 shows the experimental result. The torque is applied at $t=0.5s$ and gradually reaches its maximum value at $t=0.8s$. Due to the friction, the displacement of the poles begins only when the applied torque exceeds 30mNm. The chains are stretched due to the displacement of the poles of 58mrad and the reluctance of the system increases. Therefore, the output voltage of the measuring circuit has a peak at $t=1s$. The torque is maintained until $t=2.3s$ and the voltage becomes



(a) Rotor position and velocity



(b) Demodulator output and the applied torque

Fig. 12. Quasi-static torque detection. In (a) the torque is imposed to the handle and induces an initial displacement of 58mrad at low velocity (58mrad/s). In (b), the application of the torque is detected as an augmentation of the reluctance observed as a negative voltage. When the torque is released, the chains try to realign themselves. This is detected as a diminution of the reluctance expressed as a positive voltage. The position is measured using a resolution of 383.5 μ rad.

zero since the reluctance does not change. The observed delay is due to the transient discharge of the integrator capacitors. The torque is released at $t=2.6s$. The chains tend to realign themselves when the external force becomes zero and the reluctance decreases. As a consequence, a positive voltage appears in the measuring circuit informing that there is no more torque applied on the brake. After 2.5s, there is no displacement of the poles. As the case of the initial contact, the transitional time between 2.6s and 4s is due to the discharge delay of the integrator circuit.

7. CONCLUSION

An analysis of the assumption that the arrangement of the chain-like structures in an MR actuator has an influence on the magnetic reluctance has been described. The hypothesis has been developed using a pair of ferromagnetic particles placed in a carrier liquid. It can be concluded that when the chains operating in shear mode are stretched, the separation of the particles by the non-magnetic liquid has the effect of increasing the magnetic reluctance of the fluid gap. Considering that the chains of an MR suspension interact with the magnetic poles, the reluctance can therefore be associated to an external torque.

A rotary MR brake operating in shear mode has been used in order to investigate this hypothesis. Since the inductance of the coil is inversely proportional to the magnetic reluctance, a measure of the coil impedance is used as proof of concept. A high precision demodulator indicates the phase difference between the excitation voltage and the measured current which depends on the magnetic reluctance. Experimental results demonstrate that the reluctance of the fluid gap increases when the chains are stretched.

Although the measure of impedance is a direct indication of the reluctance, it does not provide sufficient sensibility to torque detection. The torque detection is obtained using the same brake equipped with two coils. The first coil is used to generate a constant magnetic flux. The reluctance variation can be perceived as a change in the magnetic flux. A measure of the current induced in the second coil is the image of the derivative of the reluctance.

In a preliminary test, the system reacts satisfactorily to the variation of an external torque and is able to detect the inclination of the chain before their rupture. An experimentation in a quasi-static regime highlights that the application as well as the release of a torque can also be detected due to the viscoelastic behaviour of the chains.

Two different cases are observable in this experiment. (1) When a torque is applied at the handle, the displacement of the poles stretches the chains and the reluctance of the magnetic circuit increases. The relative displacement of the poles is inversely proportional to the braking torque. As a consequence, the reluctance variation is even better measurable than as the magnetic field is weak. (2) When the torque that stretches the chains becomes zero, the interaction force between the particles, proportional to the field, tends to realign the chains to their original position and the reluctance decreases. It characterizes the elastic response of the fluid in pre-yield regime. This phenomenon is best observable when a high magnetic field strength is applied.

Similar to strain gauge-based torque transducers, the working principle of the proposed technique is based on the detection of a displacement. Indeed, the interaction forces between the particles due to the viscoelastic behaviour need to be higher than the parasitic forces characterized by viscous or coulomb friction in the rotor. Otherwise the interaction forces are not sufficient to generate a rotor displacement when it is released. Therefore, the prototype possessed no bearing and no seals.

The tests are realized in permanent regime. The excitation voltage and the braking torque, are maintained constant. When the input current is modified to control the braking torque, it naturally results in a flux variation and in an induced current in the coils. In this case, it can not be concluded if the observed output voltage is due to the reluctance variation or the variation of the current supply. Besides, the brake should be maintained under the saturation of the ferromagnetic path and under the mechanical saturation of the fluid.

This method holds great potential for the control of MR actuators in order to detect the chain rupture critical point (or pre to post-yield transition) and can be implemented as an embedded sensor to detect external forces variations.

REFERENCES

- [1] C. Rossa, J. Lozada, and A. Micaelli, "Magnetic flux analysis on magnetorheological actuators can detect external force variation," in *Sensors, 2012 IEEE*, 2012, pp. 1–4.
- [2] C. Fang, B. Y. Zhao, L. S. Chen, Q. Wu, N. Liu, and K. A. Hu, "The effect of the green additive guar gum on the properties of magnetorheological fluid," *Smart Materials and Structures*, vol. 14, no. 1, pp. N1–N5, 2005.
- [3] M. R. Jolly, J. W. Bender, and J. D. Carlson, "Properties and applications of commercial magnetorheological fluids," in *Smart Structures and Materials*, L. P. Davis, Ed., vol. 3327. SPIE, 1998, pp. 262–275.
- [4] D. Guth, D. Cording, and J. Maas, "Mrf based clutch with integrated electrical drive," in *Advanced Intelligent Mechatronics (AIM), 2011 IEEE/ASME International Conference on*, July 2011, pp. 493–498.
- [5] F. Periquet and J. Lozada, "A miniature 1-dof mr fluid based haptic interface," in *International Exhibition on Smart Actuators and Drive Systems*, 2010.
- [6] A. Grunwald and A. Olabi, "Design of magneto-rheological (mr) valve," *Sensors and Actuators A: Physical*, vol. 148, no. 1, pp. 211–223, 2008.
- [7] S. J. Dyke, B. F. Spencer, Jr., M. K. Sain, and J. D. Carlson, "An experimental study of MR dampers for seismic protection," *Smart Material Structures*, vol. 7, pp. 693–703, Oct. 1998.
- [8] C. Rossa, J. Lozada, and A. Micaelli, "Interaction power flow based control of a 1-dof hybrid haptic interface," in *Haptics: Perception, Devices, Mobility, and Communication*, ser. Lecture Notes in Computer Science, P. Isokoski and J. Springare, Eds., vol. 7283. Springer Berlin Heidelberg, 2012, pp. 151–156.
- [9] Y. Yamaguchi, J. Furusho, S. Kimura, and K. Koyanagi, "Development of High-Performance MR Actuator and its Application to 2-D Force Display," *International Journal of Modern Physics B*, vol. 19, pp. 1485–1491, 2005.
- [10] C. Rossa, J. Lozada, and A. Micaelli, "A new hybrid actuator approach for force-feedback devices," in *Intelligent Robots and Systems (IROS), 2012 IEEE/RSJ International Conference on*, 2012, pp. 4054–4059.
- [11] J. Blake and H. Gurocak, "Haptic glove with mr brakes for virtual reality," *Mechatronics, IEEE/ASME Transactions on*, vol. 14, no. 5, pp. 606–615, Oct. 2009.
- [12] J. Lozada, M. Hafez, and X. Boutillon, "A novel haptic interface for musical keyboards," in *Advanced intelligent mechatronics, 2007 IEEE/ASME international conference on*, Sept. 2007, pp. 1–6.
- [13] C. Rossa, J. Lozada, and A. Micaelli, "Stable haptic interaction using passive and active actuators," in *Robotics and Automation (ICRA), 2013 IEEE International Conference on*, 2013, pp. 2386–2392.
- [14] A. Olabi and A. Grunwald, "Design and application of magneto-rheological fluid," *Materials & Design*, vol. 28, no. 10, pp. 2658–2664, 2007.
- [15] C. Joung and H. See, "The influence of wall interaction on dynamic particle modelling of magneto-rheological suspensions between shearing plates," *Rheologica Acta*, vol. 47, pp. 917–927, 2008, 10.1007/s00397-008-0282-3.
- [16] G. Bossis, S. Laci, A. Meunier, and O. Volkova, "Magnetorheological fluids," *Journal of Magnetism and Magnetic Materials*, vol. 252, no. 0, pp. 224–228, 2002, [jce:title;Proceedings of the 9th International Conference on Magnetic Fluids;jce:title;](#)
- [17] A. K. Kwan, T. H. Nam, and Y. Y. II, "New approach to design mr brake using a small steel roller as a large size magnetic particle," in *Control, Automation and Systems, 2008. ICCAS 2008. International Conference on*, Oct. 2008, pp. 2640–2644.
- [18] C. Gordon and T. Barton, "Reluctance distribution modelling of saturated salient pole synchronous machines," *Energy Conversion, IEEE Transactions on*, vol. 9, no. 2, pp. 323–329, 1994.
- [19] D. Kittipoomwong, D. J. Klingenberg, and J. C. Ulicny, "Dynamic yield stress enhancement in bidisperse magnetorheological fluids," *Journal of Rheology*, vol. 49, no. 6, pp. 1521–1538, 2005.
- [20] W. Nassar, X. Boutillon, and J. Lozada, "Pre-yield shearing regimes of magnetorheological fluids," in *Proceedings of the ASME 2012 Conference on Smart Materials, Adaptive Structures, and Intelligent Systems*, 2012, p. 6 p. [Online]. Available: <http://hal-polytechnique.archives-ouvertes.fr/hal-00817833>
- [21] R. Tao, "Super-strong magnetorheological fluids," *Journal of Physics: Condensed Matter*, vol. 13, no. 50, p. R979, 2001.
- [22] G. M. Kamath and N. M. Wereley, "A nonlinear viscoelastic - plastic model for electrorheological fluids," *Smart Materials and Structures*, vol. 6, no. 3, p. 351, 1997.

- [23] M. R. Jolly, J. D. Carlson, and B. C. Muoz, "A model of the behaviour of magnetorheological materials," *Smart Materials and Structures*, vol. 5, p. 607, 1996.
- [24] X. Wang and F. Gordaninejad, "Flow analysis and modeling of field-controllable, electro- and magneto-rheological fluid dampers," *Journal of Applied Mechanics*, vol. 74, no. 1, pp. 13–22, 2007.
- [25] G. Yang, B. S. Jr., J. Carlson, and M. Sain, "Large-scale mr fluid dampers: modeling and dynamic performance considerations," *Engineering Structures*, vol. 24, no. 3, pp. 309 – 323, 2002.
- [26] J. de Vicente, M. T. Lpez-Lpez, J. D. G. Durn, and F. Gonzalez-Caballero, "Shear flow behavior of confined magnetorheological fluids at low magnetic field strengths," *Rheologica Acta*, vol. 44, pp. 94–103, 2004, 10.1007/s00397-004-0383-6.
- [27] W. Li and H. Du, "Design and experimental evaluation of a magnetorheological brake," *The International Journal of Advanced Manufacturing Technology*, vol. 21, pp. 508–515, 2003, 10.1007/s001700300060.
- [28] J. Huang, J. Zhang, Y. Yang, and Y. Wei, "Analysis and design of a cylindrical magneto-rheological fluid brake," *Journal of Materials Processing Technology*, vol. 129, no. 13, pp. 559 – 562, 2002, [The 10th International Manufacturing Conference in China \(IMCC 2002\)](#);